

Analysis of Particle Mobilization and Impact on Filter Performance in Drainage Tunnels

토립자 유동이 터널 배수재의 폐색에 미치는 영향 연구

Park, Kwang-Joon, 박 광 준¹⁾, Lee, In-Mo, 이 인 모²⁾

¹⁾ Executive Director, Duck-Chun Engineering Co., 덕천 엔지니어링, 전무이사

²⁾ Professor, Dept. of Civil Engineering, Korea Univ., 고려대학교 토목환경공학과 교수

개 요 : 본 논문은 지하수 흐름하에서의 풍화 잔류토의 세립자 유동특성을 파악하기 위한 수치모델을 개발하고, 실내에서 실시한 수리 모형실험을 통하여 수치모델의 적합성을 규명하였다. 한국의 풍화 잔류토는 점토와 모래의 중간 상태의 특성을 보이는 관계로 기존의 토립자 유동모델중 점토 또는 모래에 적합한 모델에 의해서는 정확한 유동특성의 파악에 한계가 있었다. 따라서, 본 연구에서는 한국의 풍화 잔류토에 적합한 세립자 유동모델을 제시함으로써 풍화 잔류토를 대상으로 시공되는 굴토공사, 댐 축조공사, 그리고 터널공사시 지하수 유입에 따른 세립토사의 유실특성을 이론적으로 규명하였고, 현장에서 배수재로 광범위하게 쓰이고 있는 토목섬유인 부직포의 투수 및 배수특성을 검토하였다.

주요어 : 토립자 유동, 한계 전단 응력, 토립자의 이탈, 이동, 집적, 폐색

1. INTRODUCTION

The objectives of this research are to evaluate hydraulic behavior and particle transport and filtration performance of the combined system of the weathered residual base soil and nonwoven geotextile filter layer, and to propose a new filter design concept for nonwoven geotextile which is used as filter (or drainage) material for a drainage tunnel in weathered residual soils.

In this study, a physical model for soil particle erosion, migration, deposition and clogging phenomena is suggested based on the mass balance theory. The model suggested can be applied to one dimensional flow perpendicular to the base soil-filter system. In addition, an analytical transmissivity prediction model considering time dependant filter clogging in drainage tunnels are suggested. Filter clogging effects by fine particles may be evaluated not only by the soil retention in the geotextile layer, but also by the pressure drop or permeability reduction in the soil-geotextile composite system.

2. Development of Mathematical Model

2.1 Governing Equations of Flow and Transport

A section of the soil column from the back of the tunnel lining through which seepage is taking place is taken and shown in Fig. 1. This section is composed of a base soil-geotextile system which has the initial permeability, K_0 , and the initial porosity, n_0 . The section is cylindrical with a cross-sectional area, A_r (cm^2), and total length, L (cm). Assuming that Darcy's law is valid, the

initial flow rate, q_0 , is expressed as:

$$q_0 = \frac{K_o}{\mu} A_r \frac{\Delta p}{L} \quad (1)$$

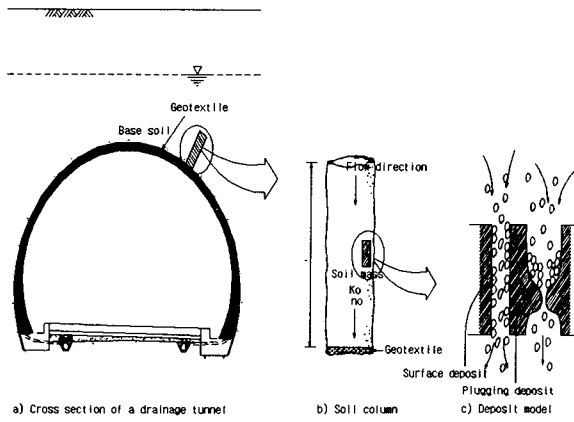


Figure 1 Particle transport model of soil-geotextile system in a drainage tunnel

Considering the mass balance of fine particles in an elemental volume, the governing equation for particle transport may be written as:

$$-\frac{\partial}{\partial t}(nC + n_0\sigma) + V\frac{\partial C}{\partial x} = 0 \quad (2)$$

where, nC = volume of fines in suspension,
 $n_0\sigma$ = volume of fines deposited,
 x, t = space and time coordinates.

Using $n_0(1-\sigma)$ for n , the equation becomes:

$$n_0(1-\sigma)\frac{\partial C}{\partial t} + n_0\frac{\partial \sigma}{\partial t} + V\frac{\partial C}{\partial x} = 0 \quad (3)$$

and, if both σ and C are small compared to unity, this is well approximated by:

$$\frac{\partial C}{\partial t} + V\frac{\partial C}{\partial x} + \frac{\partial \sigma}{\partial t} = 0 \quad (4)$$

To complete this theoretical description, a local deposition and entrainment law gives $\partial \sigma / \partial t$ as a function of C , σ , and V . The third term in Eq. 4 is a key factor accounting for the processes of particle detachment and deposition.

2.2 Local Laws for Deposition and Entrainment

To determine the critical velocity and the critical pressure of the weathered residual soil, both rapid flow-increase case and rapid pressure-increase case are assumed. A new relationship between

erosion rate and critical shear stress of the weathered residual soils is shown below:

i) For rapid flow-increase case

$$\begin{aligned}\frac{\partial \sigma}{\partial t} &= -\beta_r V_c - \beta_c (V - V_c) & ; & \quad V \geq V_c \\ \frac{\partial \sigma}{\partial t} &= -\beta_r V & ; & \quad V < V_c\end{aligned}\quad (5a)$$

where, β_r, β_c = erosion rate, and
 V_c = critical fluid velocity.

ii) For rapid pressure-increase case

$$\begin{aligned}\frac{\partial \sigma}{\partial t} &= -\alpha_r P_c - \alpha_c (P - P_c) & ; & \quad P \geq P_c \\ \frac{\partial \sigma}{\partial t} &= -\alpha_r P & ; & \quad P < P_c\end{aligned}\quad (5b)$$

where, P = hydraulic pressure,
 P_c = critical hydraulic pressure, and
 α_r, α_c = erosion rates.

A finite difference scheme is used to solve this system numerically under the following initial and boundary conditions.

$$\begin{aligned}C(x, 0) &= 0.0 & ; & \quad P(x, 0) = 0.0 & ; & \quad V(x, 0) = 0.0 \\ \frac{\partial C(L, t)}{\partial x} &= 0.0 & ; & \quad \frac{\partial P(L, t)}{\partial x} = 0.0 & ; & \quad \frac{\partial V(L, t)}{\partial t} = 0.0\end{aligned}\quad (6)$$

The rate of effluent concentration at the end of soil-geotextile column, considering boundary conditions, can be calculated from the following equation:

i) For velocity-controlled test conditions,

$$\begin{aligned}\frac{\partial C}{\partial t} &= \alpha_r P_c + \alpha_c (P - P_c) - \lambda C & ; & \quad V \geq V_c \\ \frac{\partial C}{\partial t} &= \alpha_r P - \lambda C & ; & \quad V < V_c\end{aligned}\quad (7a)$$

ii) For pressure-controlled test conditions,

$$\begin{aligned} \frac{\partial C}{\partial t} &= \beta_r V_c + \beta_c (V - V_c) - \lambda C & ; & \quad P \geq P_c \\ \frac{\partial C}{\partial t} &= \beta_r P - \lambda C & ; & \quad P < P_c \end{aligned} \quad (7b)$$

Based on the new concept of critical shear stress in weathered residual soils, the correlation between erosion rate and shear stress is expressed. And to account for the particle deposition mechanisms and to obtain a closed-form expression for λ , a trial and error method is adapted.

3. Preparation of Soil and Geotextile Samples

3.1 Soil Samples

Two types of typical Korean weathered residual soils are chosen for this research: the one is more like a cohesive soil sampled from the Poi-dong area (named 'P-soil' hereafter); the other is more or less a cohesionless soil from the Shinnae-dong area (named 'S-soil' hereafter) in Seoul. A series of soil classification tests is performed again to confirm the stated properties and the main characteristics are summarized in Table 1.

Table 1 Index properties of selected residual soils

Soil sample	w (%)	LL (%)	PL (%)	PI (%)	FC* (%)	Gs	USCS
Poi-dong	16.5	34.0	19.8	14.2	47.4	2.74	SC
Shinnae-dong	10.0	NP	NP	NP	10.1	2.63	SW-SM

Note: FC* = Fine Content (d < 0.074mm)
NP = non plastic

The compaction results for each soil sample is summarized in Table 2.

Table 2 Compaction results for the soil samples

Soil Sample	OMC (%)	γ_{dmax} (t/m ³)	Ws (g)	Ww (g)	n _o (%)	K _o (cm/sec)
P-soil	16.5	1.76	791.68	130.63	41.63	1.8*10 ⁻⁴
S-soil	10.0	1.89	841.50	84.15	35.36	5.0*10 ⁻³

The compacted soil samples are saturated by soaking in water for 24 hours under the 10cm of water head (achieved more than 95% of saturation) to achieve reliable measurements of the pore pressure response and permeability changes.

3.2 Geotextile Samples

Two types of nonwoven geotextiles which are most widely used in filtration applications are chosen for this study: one is the most frequently used filter material, 2.69mm thick and 311.2g/m², and denoted NW-1 in this paper; the other is 4.83mm thick and 551.0g/m², and named NW-2. Properties of the two different geotextiles are identified as shown in Table 3.

Table 3 Typical range of selected non-woven geotextile properties

Geotextile Types	Thickness t _g , (mm)	Weight μ _g , (g/m ²)	Porosity n _g , (%)	AOS (μ m)	FOS (μ m)	Permeability Kg, (cm/sec)
NW-1	2.69	311.2	91.4	180	103	0.21
NW-2	4.83	551.0	91.5	170	100	0.39

The selected geotextiles are prepared as 10cm diameter disks. Prior to the laying down of the geotextile disk under the cylinder cell, the prepared geotextile disk is weighed in dry conditions and then it is saturated in boiled water to remove air trapped in void space.

3.3 Test Equipment Set-Up

The modified KUGRC gradient-ratio test is devised to measure the seepage force at the bottom of the geotextile by installing a bearing plate under the geotextile, which may modify the development of the seepage force on the tunnel lining in a drainage tunnel(See Photo 1).

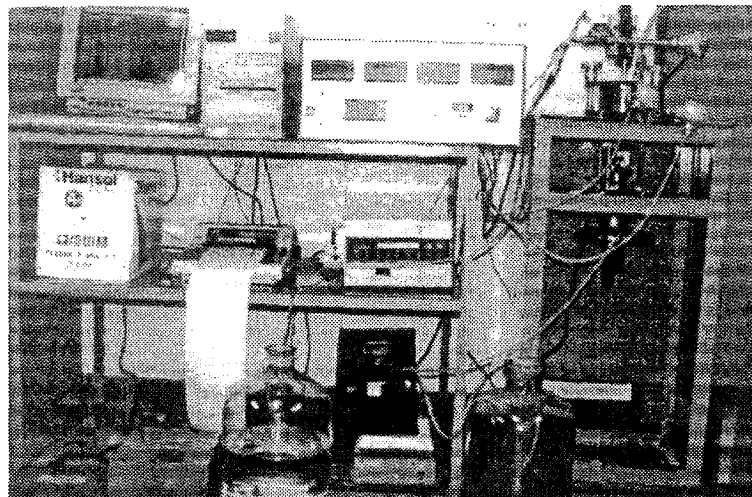


Photo 1 Picture of the modified KUGRC gradient-ratio test apparatus

4. TEST RESULTS AND DISCUSSIONS

4.1 Determination of Erosion Rate and Critical Shear Stress

The erosion rate and initial critical hydraulic pressure of the P and S-soil are determined from the rapid pressure-increase and velocity-increase test as shown in Fig. 1 and 2.

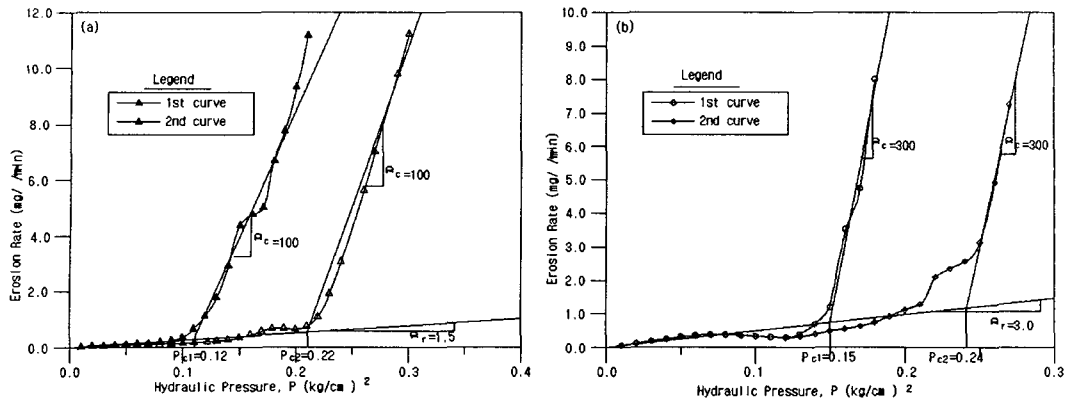


Figure 1 Results of the rapid pressure-increase test: (a) P-soil; (b) S-soil

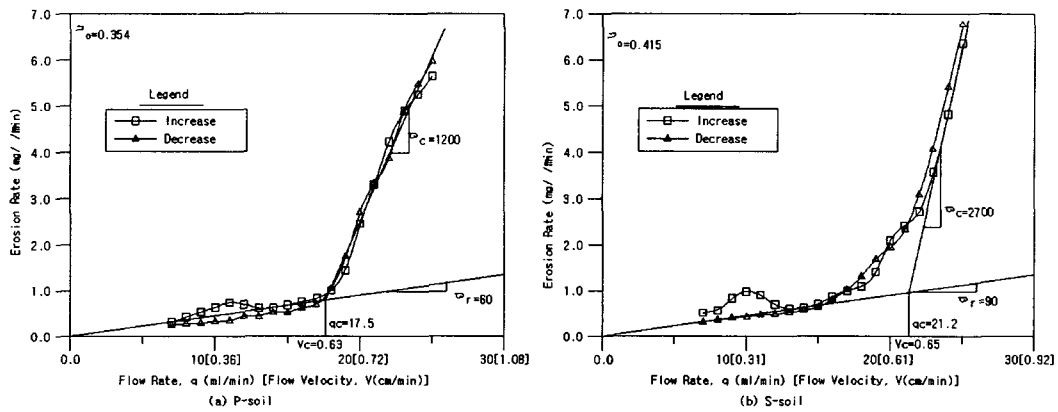


Figure 2 Results of the rapid velocity-increase test: (a) P-soil; (b) S-soil

4.2. Results of Velocity-Controlled Filtration Test

In the velocity-controlled filtration tests, three flow rates, $q = 7, 14$ and 21 ml/min , are applied. The range of flow rates is determined from the results of pilot test for the compacted soil samples. The seepage velocities calculated from each flow rate are $V = 0.216, 0.432$ and 0.648 cm/min , respectively. The results of velocity-controlled filtration test depending on the flow rates and the time intervals are shown in Fig. 3.

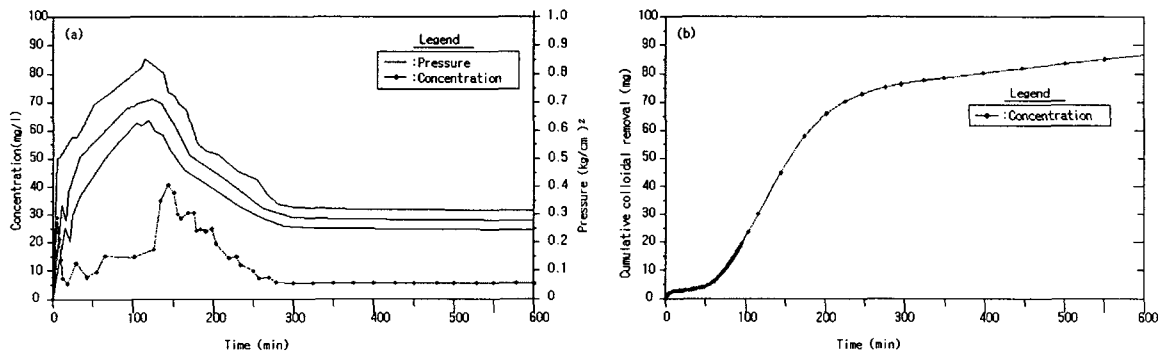


Figure 3 Concentration-time curves for the P-soil under the velocity-controlled test; (a) concentration and pressure; (b) cumulative colloidal removal

4.3 Results of Hydraulic Pressure-Controlled Filtration Test

In hydraulic pressure-controlled filtration tests, three hydraulic heads, $H_d = 0.3, 0.6$ and 0.9m ($P = 0.03, 0.06$ and 0.09kg/m^2 , respectively) are chosen to be applied. Flow rate and effluent concentration are measured during the testing period. Based on the relationship between erosion rate and applied pressure from the rapid hydraulic pressure-increase tests, the critical hydraulic pressure of the P and S-soil are $P_c = 0.12\text{kg/m}^2$ and 0.15kg/cm^2 , respectively. Fig. 4 shows the variation of flow rates and concentrations under the condition of the pressure-controlled tests.

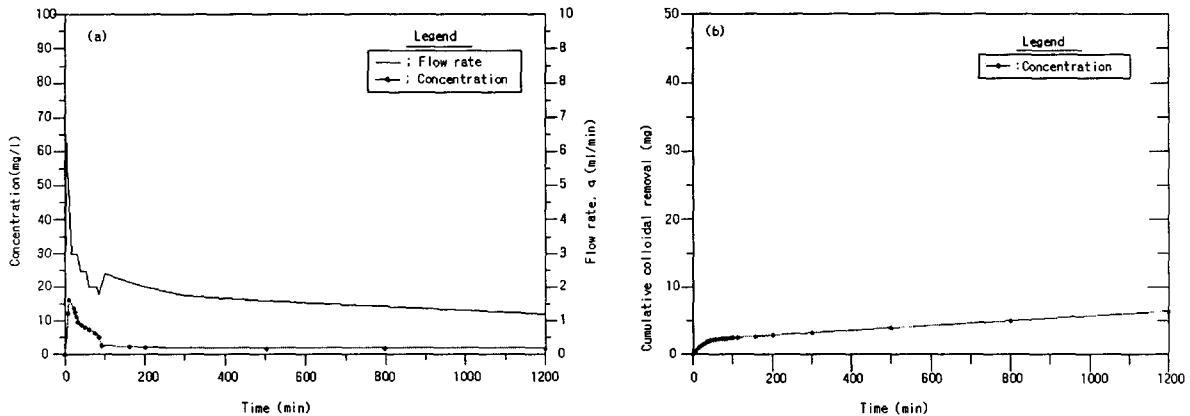


Figure 4 Concentration-time curves for P-soil under the pressure controlled test; (a) concentration and flow rate; (b) cumulative colloidal removal

4.4 Comparison with Theoretical Solutions

As shown in Fig. 5, the measured effluent concentrations coincided with the theoretically calculated using $\lambda = 1.8\text{min}^{-1}$.

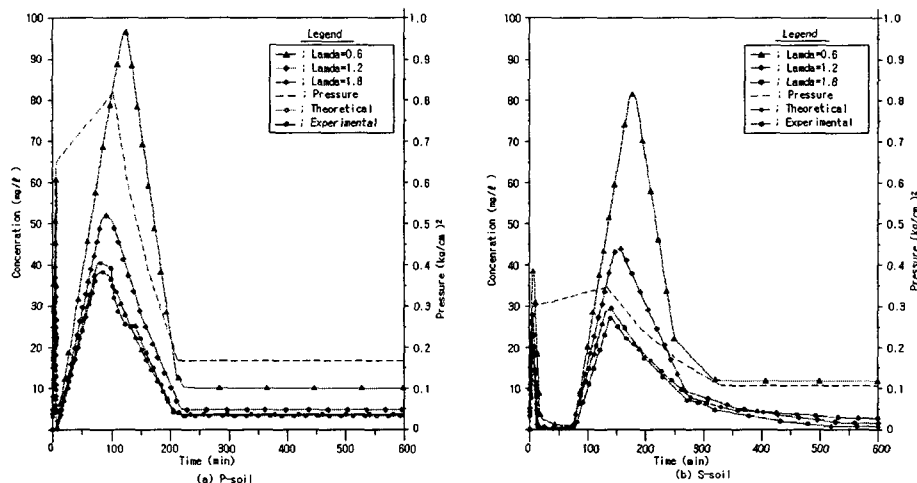


Figure 5 Comparison of experimental and theoretical concentrations for the velocity-controlled test

5. Conclusions

The following conclusions may be drawn from the interpretation of gradient ratio test data presented for non-woven geotextiles and the weathered residual soils used in experiments.

- (1) A new definition on the critical shear stress of weathered residual soil as the corresponding pressure of the cross point between lower and steeper slopes of erosion rate is suggested.
- (2) Under the velocity-controlled condition, pressure drop in the soil-geotextile system reaches about 50 to 60% of peak value within 24 hours. And under pressure-controlled condition, flow reduction is observed to be 30 to 60 %.
- (3) Test results reveal that the initial GR-value never shows $GR = 1.0$ due to initial turbulence effects and non homogeneity of soil sample. Therefore, the ratio GR_f/GR_i is recommended to evaluate long-term compatibility of soil-geotextile system.
- (4) At the end of the filtration test, it is found that about 0.1% of the total soil mass is retained in geotextile layer, and 10% of them is washed out through the geotextile filter layer.
- (5) For both of the P and S-soil and geotextile sample, NW-1, the calculated concentration using $\lambda = 1.8\text{min}^{-1}$ shows good agreement with the test results.
- (6) Being confined by external pressure and clogged by fine particles, permeability of geotextile drainage layer is reduced to be one-third of the initial permeability of clean filter, especially in a drainage tunnel constructed in water-bearing weathered residual soil.
- (7) At the first filling of ground water table after construction of a drainage tunnel, which exceeds the critical hydraulic pressure, $P = 0.12\text{-}0.15\text{kg/cm}^2$, the retained soil mass in the geotextile drainage is estimated to be 565-1130g/m and the passed soil mass is 10-20g/m in a 3m-radius drainage tunnel.
- (8) It is observed that one thin layer of geotextile drainage filter is not enough to evacuate seepage water without restriction. To discharge the inflow water freely to the side-wall pipe, 10 to 15 layers of thin geotextile or a thick and stiff geosynthetic or a geocomposite layer is required.

ACKNOWLEDGEMENT

This research is supported by the Ministry of Construction and Transportation of Korea (R&D/96-0046).

REFERENCES

1. Lee, I. M., Kim, S. K., and Kim, H. S. (1988). "An experimental study on filter clogging due to particle transport of weathered residual soils", Proceedings of the KGS spring '98 National Conference, pp. 93-100.
2. Lee, I. M., Park, K. J., and Kim, H. S. (1998). "An experimental study on clogging effects of soil filter materials", Proceedings of the KGS autumn '98 National Conference, pp. 65-72.
3. Lee, I. M., Park, K. J., and Yoo, S. H. (1998). "An experimental study of filter clogging for the in-plane flow of residual soils", Proceedings of the KGS autumn '98 National Conference, pp.73-80.
4. Lee, I. M., Yoo, S. H., Park, K. J., and Reddi, L. N. (1999). "Clogging phenomena and water carrying capacity of a tunnel drainage system", Proceedings of the World Tunnel Congress '99.